Accepted Manuscript

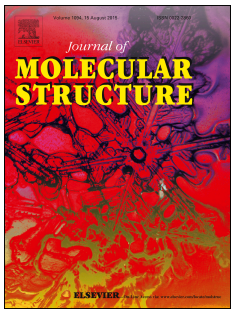

Synthesis, bioactivities, DFT and *in-silico* appraisal of azo clubbed benzothiazole derivatives

Chaitannya W. Ghanavatkar, Virendra R. Mishra, Suraj N. Mali, Hemchandra K. Chaudhari, Nagaiyan Sekar

PII: S0022-2860(19)30534-4

DOI: https://doi.org/10.1016/j.molstruc.2019.04.123

Reference: MOLSTR 26495

To appear in: *Journal of Molecular Structure*

Received Date: 30 January 2019

Revised Date: 3 April 2019

Accepted Date: 28 April 2019

Please cite this article as: C.W. Ghanavatkar, V.R. Mishra, S.N. Mali, H.K. Chaudhari, N. Sekar, Synthesis, bioactivities, DFT and *in-silico* appraisal of azo clubbed benzothiazole derivatives, *Journal of Molecular Structure* (2019), doi: https://doi.org/10.1016/j.molstruc.2019.04.123.

Synthesis, Bioactivities, DFT and *in-silico* appraisal of azo clubbed Benzothiazole derivatives.

Chaitannya W. Ghanavatkar[a], Virendra R. Mishra, Suraj N. Mali[b], Hemchandra K. Chaudhari[b], Nagaiyan Sekar[a,*]

Chaitannya W. Ghanavatkar -ORCID ID- https://orcid.org/0000-0003-0821-1083

Virendra R. Mishra -ORCID ID- https://orcid.org/0000-0003-0070-4705

[a,*]Department of Dyestuff Technology, Institute of Chemical Technology, Matunga (E), Mumbai, Maharashtra, India, PIN: 400 019.

E-mail: nethi.sekar@gmail.com; n.sekar@ictmumbai.edu.in

ORCID ID- https://orcid.org/0000-0001-7568-5129

Suraj Narayan Mali -ORCID ID- https://orcid.org/0000-0003-1995-136X

[b]Department of Pharmaceutical Sciences and Technology, Institute of Chemical Technology, Matunga (E), Mumbai, Maharashtra, India, PIN: 400 019.

E-mail: hemchandrachaudhari@yahoo.com, hk.chaudhari@ictmumbai.edu.in

ORCID ID- https://orcid.org/0000-0001-6866-9147

Graphical Abstract:

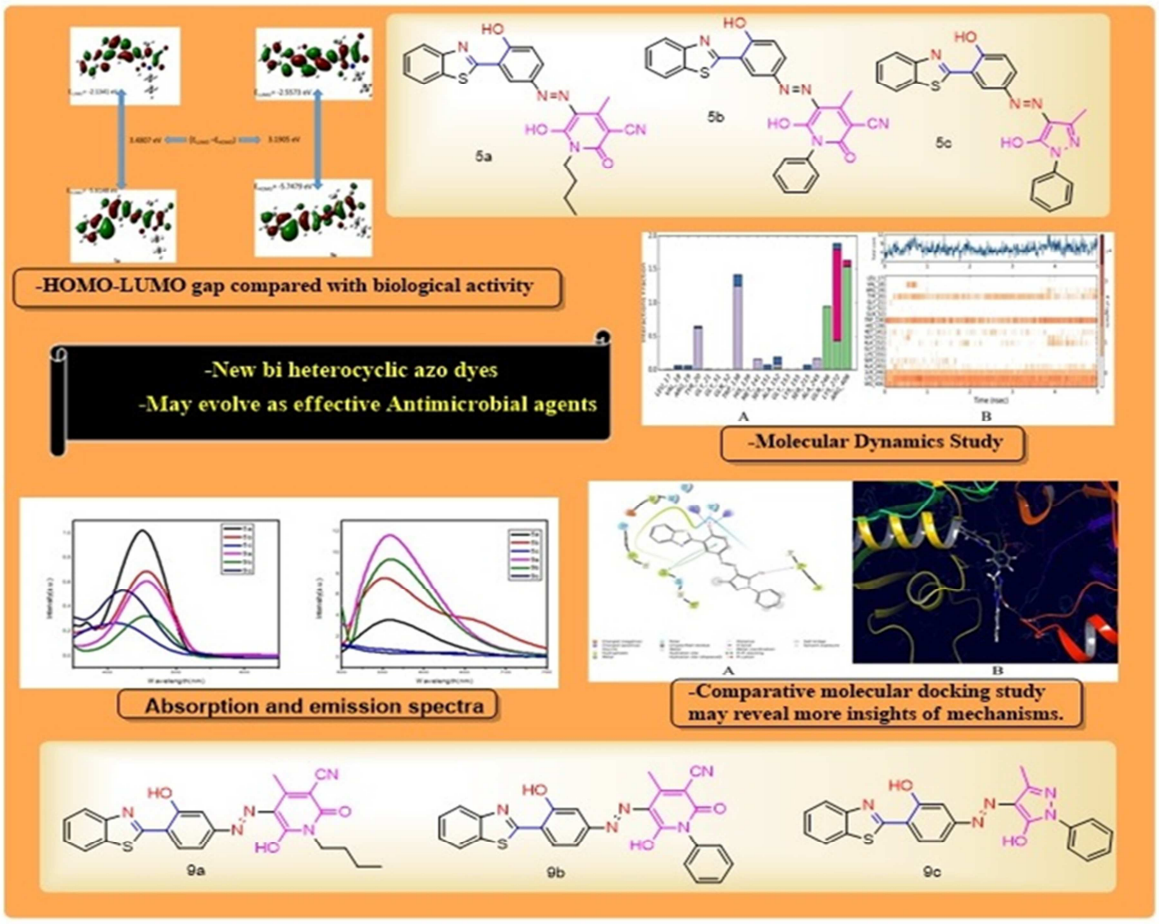

Abstract

Six new azo clubbed benzothiazole dyes were synthesized by diazotization reaction. These six novel compounds were characterized using ^{1}H NMR, FTIR, UV–Visible, fluorescence spectroscopy, LC-MS, and elemental analysis. The *in-vitro* antimicrobial screening studies were performed using popular REMA assay method on "gram-positive" ("*Staphylococcus aureus")* and "gram-negative" ("*Escherichia coli"*) strains. DNA cleavage study was also carried out to check nuclease activity. The "HOMO-LUMO" theoretical calculations were correlated with current *in-vitro* antibacterial results. *In -silico* studies were performed using Molecular Docking, Molecular dynamics, Prime MMGBSA, admetSAR, and QikProp ADMET method.

Keywords: Benzothiazole**,** azo clubbed heterocycles, biological activity**,** Molecular docking**,** Density functional theory (DFT)

1. Introduction

Since the last couple of decades, S and N containing heterocycles i.e. Benzothiazole, thiazole, isothiazole scaffolds attracted researchers and utilized in dyeing on polyester fiber[1,2], nonlinear optical materials (NLO) [3], structural and spectroscopic properties, ESIPT and DFT studies[4,5], antimycobacterial [6], antimicrobial [7], anticancer [8] and various pharmacological activities[9]. Furthermore, pyridone and pyrazole containing compounds also play an important role in medicinal chemistry [10–15].

Among these compounds, Heterocyclic azo dyes can be easily produced and comprise an important class of aromatic compounds[1,16–20]. Azo dyes are also involved in biological reactions like RNA inhibition, nitrogen fixation, protein synthesis [21]. Various azo dyes containing either metal complex or heterocyclic ring are synthesized and tested for in vivo and in vitro activity[22–24]. An azo compound Sulfasalazine is a well-known antibiotic in human infections have great importance, as sulfonamides are derived from “protonsil”. However, Antimicrobial drug resistance to antibiotics is a widespread problem. Hence design, synthesis, and testing of new compounds are necessary.

In this regard, we designed, synthesized and screened the biological activity of six new benzothiazole containing heterocyclic azo dyes. Dyes are synthesized through azo coupling reaction using substituted pyridone or substituted pyrazole as coupling component.
The newly synthesized heterocyclic azo dyes are investigated for their potential *in-vitro* activities against both, “gram-positive” i.e. *“S. aureus” (“Staphylococcus aureus”)* and “gram-negative” bacteria i.e. *“E. Coli” (“Escherichia Coli”)* strains by using “REMA method”. DNA cleavage activity studies were carried out using the electrophoretic mobility shift assay. “HOMO-LUMO” gap of all the compounds were calculated using the computational method and used to compare with the actual *in-vitro* antibacterial results.
The molecular docking simulations were performed for three bacterial targets including the common one. Using Molecular docking study, the binding affinities were determined [25] against the variety of targets and might reveal more insights into the possible mechanisms.

2. Experimental

2.1 Materials and equipment

Solvents and chemicals were obtained from the commercial source (“Spectrochem” and “SD Fine Chemicals Ltd”.) and then used for the experiments with no further purification. Reactions were monitored by using thin layered chromatography plates (TLC) (0.25mm “E-

Merck silica gel 60-F254, pre-coated"). TLC plates were visualized using UV light. Standard melting point apparatus used from "Sunder industrial product, Mumbai" to analyze melting points. "Nuclear magnetic resonance (^{1}H NMR)" spectra recorded using 400MHz or 500MHz instrument of "Agilent Technology". "FT-IR" spectrum recorded on "Perkin Elmer Fourier Transform IR instrument". "Perkin Elmer Lambda-25 spectrophotometer" was used to record the absorption spectra of all the compounds at room temperature (25-27 ^{o}C). Fluorescence spectra are recorded with "Varian Cary Eclipse fluorescence spectrophotometer" at room temperature. The LC-MS of the compounds were measured on Varian Inc. mass analyzer (410 Prostar Binary LC with 500 MS IT model) with Electrospray Ionization (ESI, negative mode).

2.2 Computational Method

"Density Functional Theory (DFT)" was used to optimize the ground state of all compounds by using the "Gaussian 09 package" [26] and popular "hybrid functional B3LYP". The B3LYP functional is a combination of "Becke's three parameter exchange functional (B3)" [27] with the "nonlocal correlation functional of Lee, Yang, and Parr (LYP)" [28]. The basis sets used for all atoms were the popular Pople's split-valence basis sets. The B3LYP functional is used with the "double zeta basis set 6-31G (d)" for optimization. Molecules are optimized in the gas phase using the same basis sets.

2.3 Molecular Modelling

The popular Glide module from Schrodinger's molecular modeling package was utilized for calculations of molecular dockings. Molecular dynamics for 1.2ns was done using Desmond module incorporated in Schrodinger's molecular modeling package 2017 [29]. All properties corresponding with calculations of ADME were calculated using the QikProp [30] module (QikProp, Schrodinger LLC, NY, 2017). The molecular mechanics generalized born surface area energies (MM GBSA) were also calculated using the Prime module [31].

2.4 Biological activities

2.4.1 Antibacterial activities

The newly synthesized azo compounds were checked for their antimicrobial activity by using the "REMA" ("Resazurin microtiter assay method") on "gram-positive", *"S. aureus"* (*"Staphylococcus aureus")* and "gram-negative", *"E. Coli"* (*"Escherichia coli"*) bacterial strains. The activities are reported in "Minimum inhibitory concentration (MIC in µg/mL)" form. Detail procedure is given in Supplementary Information (SI).

2.4.2 DNA cleavage studies

DNA cleavage studies carried out with the plasmid pBR 322 DNA using the Electrophoretic mobility shift assay. Detail procedure is given in Supplementary Information (SI).

2.5 Synthesis

Intermediates (**3, 7)** [32] and (**C1, C2)** [33] were synthesized as reported. **(C3)** used as it is received from a commercial source.

2.5.1 General procedure for preparation of intermediates 4 and 8

Substituted aromatic amine- **3** or **7** (2 mmol.) was stirred in 30% or 70% H_2SO_4. The obtained reaction mixture then cooled to 0-5 ^oC. A solution of $NaNO_2$ (2.2 mmol) prepared in water and added dropwise over the period of 15 min at 0-5 ^oC. The resulting reaction mixture was stirred for 1.5 h at 0-5 ^oC. Completion of diazotization was monitored by using starch-iodide paper. 0.01 g of urea was added to consume an excess of nitrous acid. Resulting diazonium salt solution was then immediately used for the coupling reaction with **C1** or **C2** or **C3**.

2.5.2 General procedure for synthesis of heterocyclic azo dyes 5 (a-c) and 9 (a-c)

C1 or **C2** or **C3** (2 mmol.) dissolved in a stirred solution of NaOH (2 mmol.). A clear pale yellow solution obtained is then cooled to 0-5 ^oC. To this solution, diazotized amine was added slowly, dropwise with mechanical stirring by maintaining temperature at 0-5 ^oC. Saturated sodium carbonate solution was added simultaneously to maintain pH of reaction mixture at 7–9. The solution was stirred for 2 h., before diluting or raising to neutral pH. The resulting dyes **5(a-c)** and **9(a**-c) are then filtered, washed with water, and recrystallized using ethanol. **Scheme A** represents the synthesis of new azo dyes.

2.5.2.1 Synthesis of 5-((3-(Benzo[d]thiazol-2-yl)-4-hydroxyphenyl)diazenyl)-1-butyl-6-hydroxy-4-methyl-2-oxo-1,2-dihydropyridine-3-carbonitrile (**5a**). Brown-Red solid.Yield:85 %, **m.p.=**310-312 °C **IR** (υ cm^{-1}) 3270 (OH), 2227 (CN), 1512(-N=N-) **^{1}H NMR** (500 MHz, DMSO-d^6) δ 14.76 (s, 1H), 11.93 (s, 1H), 8.45 (d, *J* = 2.2 Hz, 1H), 8.12 (d, *J* = 7.9 Hz, 1H), 8.04 (d, *J* = 8.1 Hz, 1H), 7.74 (d, *J* = 9.0 Hz, 1H), 7.54 (t, *J* = 7.3 Hz, 1H), 7.44 (t, *J* = 7.6 Hz, 1H), 7.14 (d, *J* = 8.9 Hz, 1H), 3.80 – 3.75 (m, 2H), 2.48 (s, 3H), 1.51 (m, *J* = 14.7, 7.4 Hz, 2H), 1.29 (m, *J* = 14.8, 7.4 Hz, 2H), 0.89 (t, *J* = 7.4 Hz, 3H). **LC–MS**: m/z =458.1, $[M–H]^-$. **Elemental analysis** Anal. Calcd for $C_{24}H_{21}N_5O_3S$ C, 62.73; H, 4.61; N, 15.24; found C, 62.76; H, 4.61; N, 15.25

2.5.2.2 Synthesis of 5-((3-(Benzo[d]thiazol-2-yl)-4-hydroxyphenyl) diazenyl)-6-hydroxy-4-methyl-2-oxo-1-phenyl-1,2-dihydropyridine-3-carbonitrile (5b). Brown solid, Yield: 83%, **m.p.=** 298-300 °C, **IR** (υ cm^{-1}) 3573(OH), 2219 (CN), 1508(-N=N-) **^{1}H NMR** (400

MHz, DMSO-d^6) δ 14.62 (s, 1H), 11.94 (s, 1H), 8.43 (s, 1H), 8.11 (d, *J* = 7.6 Hz, 1H), 8.00 (d, *J* = 7.6 Hz, 1H), 7.71 (d, *J* = 5.9 Hz, 1H), 7.56 – 7.34 (m, 5H), 7.27 (d, *J* = 7.2 Hz, 2H), 7.13 (d, *J* = 8.9 Hz, 1H), 2.47 (s, 3H). **LC–MS**: m/z =478.0, $[M–H]^-$. **Elemental analysis** Anal. Calcd for $C_{26}H_{17}N_5O_3S$ C, 65.12; H, 3.57; N, 14.61 found C, 65.15; H, 3.57; N, 14.62

2.5.2.3 Synthesis of 4-((3-(Benzo[d]thiazol-2-yl)-4-hydroxyphenyl)diazenyl)-3-methyl-1-phenyl-1H-pyrazol-5-ol (5c). Brown solid. Yield: 82%, **m.p. =** 226-228°C, **IR** (υ cm^{-1}) 3594(OH), 3064 (Ar-CH), 1547 (-N=N-) **^{1}H NMR** (400 MHz, DMSO-d^6) δ 13.52 (s, 1H), 11.77 (s, 1H), 8.53 (s, 1H), 8.19 (d, *J* = 7.8 Hz,1H), 8.12 (d, *J* = 8.0 Hz, 1H), 7.96 (d, *J* = 8.0 Hz, 2H), 7.75 (d, *J* = 8.6 Hz, 1H), 7.58 (t, 1H), 7.48 (t, *J* = 7.5 Hz, 3H), 7.30 – 7.15 (m, *J* = 14.9, 8.0 Hz, 2H), 2.36 (s, 3H). **LC–MS**: m/z =426.0, $[M–H]^-$. **Elemental analysis** Anal. Calcd. for $C_{23}H_{17}N_5O_2S$: C, 64.62; H, 4.01; N, 16.38; found C, 64.67; H, 4.01; N, 16.38

2.5.2.4 Synthesis of 5-((4-(Benzo[d]thiazol-2-yl)-3-hydroxyphenyl)diazenyl)-1-butyl-6-hydroxy-4-methyl-2-oxo-1,2-dihydropyridine-3-carbonitrile (9a). Red-orange solid, Yield: 87% **m. p.=**300-302°C, **IR** (υ cm^{-1}) 3578 (OH), 2226 (CN), 1506 (-N=N-) **^{1}H NMR** (400 MHz, DMSO-d^6) δ 14.42 (s, 1H), 11.94 (s, 1H), 8.23 (d, *J* = 8.7 Hz, 1H), 8.10 (d, *J* = 7.8 Hz, 1H), 8.01 (d, *J* = 8.1 Hz, 1H), 7.54 – 7.47 (m, 1H), 7.45 – 7.38 (m, 1H), 7.37 – 7.28 (m, *J* = 13.6, 7.1 Hz, 2H), 3.80 (t, 2H), 2.51 (s, 3H), 1.56 – 1.45 (m, 2H), 1.34 – 1.23 (m, 2H), 0.88 (t, 3H). **LC–MS**: m/z =458.2, $[M–H]^-$. **Elemental analysis** Anal. Calcd. for $C_{24}H_{21}N_5O_3S$ C, 62.73; H, 4.61; N, 15.24; found: C, 62.78; H, 4.66; N, 15.25

2.5.2.5 Synthesis of 5-((4-(Benzo[d]thiazol-2-yl)-3-hydroxyphenyl)diazenyl)-6-hydroxy-4-methyl-2-oxo-1-phenyl-1,2-dihydropyridine-3-carbonitrile (9b). Red solid**,** Yield: 91% **m. p.** = 286-287°C, **IR** (υ cm^{-1}) 3565 (OH), 3071 (Ar-CH), 2225 (CN), 1513(-N=N-), **^{1}H NMR** (400 MHz, DMSO-d^6) δ 14.17 (s, 1H), 11.81 (s, 1H), 8.10 (d, *J* = 8.6 Hz, 1H), 7.97 (d, *J* = 7.8 Hz, 1H), 7.88 (d, *J* = 8.1 Hz, 1H), 7.37 (s, 1H), 7.36 (d, *J* = 1.9 Hz, 1H), 7.34 (s, 1H), 7.33 – 7.31 (m, 1H), 7.30 (d, *J* = 3.4 Hz, 1H), 7.24 (d, *J* = 1.9 Hz, 1H), 7.21 (d, *J* = 2.2 Hz, 1H), 7.17 (d, *J* = 1.5 Hz, 1H), 7.16 (d, *J* = 1.7 Hz, 1H), 2.48 (s, 3H). **LC–MS**: m/z =478.0, $[M–H]^-$. **Elemental analysis** Anal. Calcd for $C_{26}H_{17}N_5O_3S$ C, 65.12; H, 3.57; N, 14.61 found: C, 65.15; H, 3.57; N, 14.62

2.5.2.6 Synthesis of 4-((4-(Bsenzo[d]thiazol-2-yl)-3-hydroxyphenyl)diazenyl)-3-methyl-1-phenyl-1H-pyrazol-5-ol (9c). Brown solid. Yield:85% **m. p. =**215-217 °C, **IR** (υ cm^{-1}) 3569(OH), 3064 (Ar-CH), 1540(-N=N-) **^{1}H NMR** (400 MHz, DMSO-d^6) δ 13.27 (s, 1H), 11.94 (s, 1H), 8.28 (d, *J* = 8.7 Hz, 1H), 8.15 (d, *J* = 8.0 Hz, 1H), 8.06 (d, *J* = 8.0 Hz, 1H), 7.94 (d, *J* = 7.9 Hz, 1H), 7.58 – 7.53 (m, 1H), 7.52 – 7.43 (m, 3H), 7.34 (d, *J* = 1.8 Hz, 1H), 7.31 (d, *J* = 2.0 Hz, 1H), 7.29 (d, *J* = 2.1 Hz, 1H), 7.25 (t, 1H), 2.35 (s, 3H). **LC–MS**: m/z

=426.0, $[M–H]^-$. **Elemental analysis** Anal. Cald. for $C_{23}H_{17}N_5O_2S$ C, 64.62; H, 4.01; N, 16.38; found C, 64.64; H, 4.01; N, 16.39

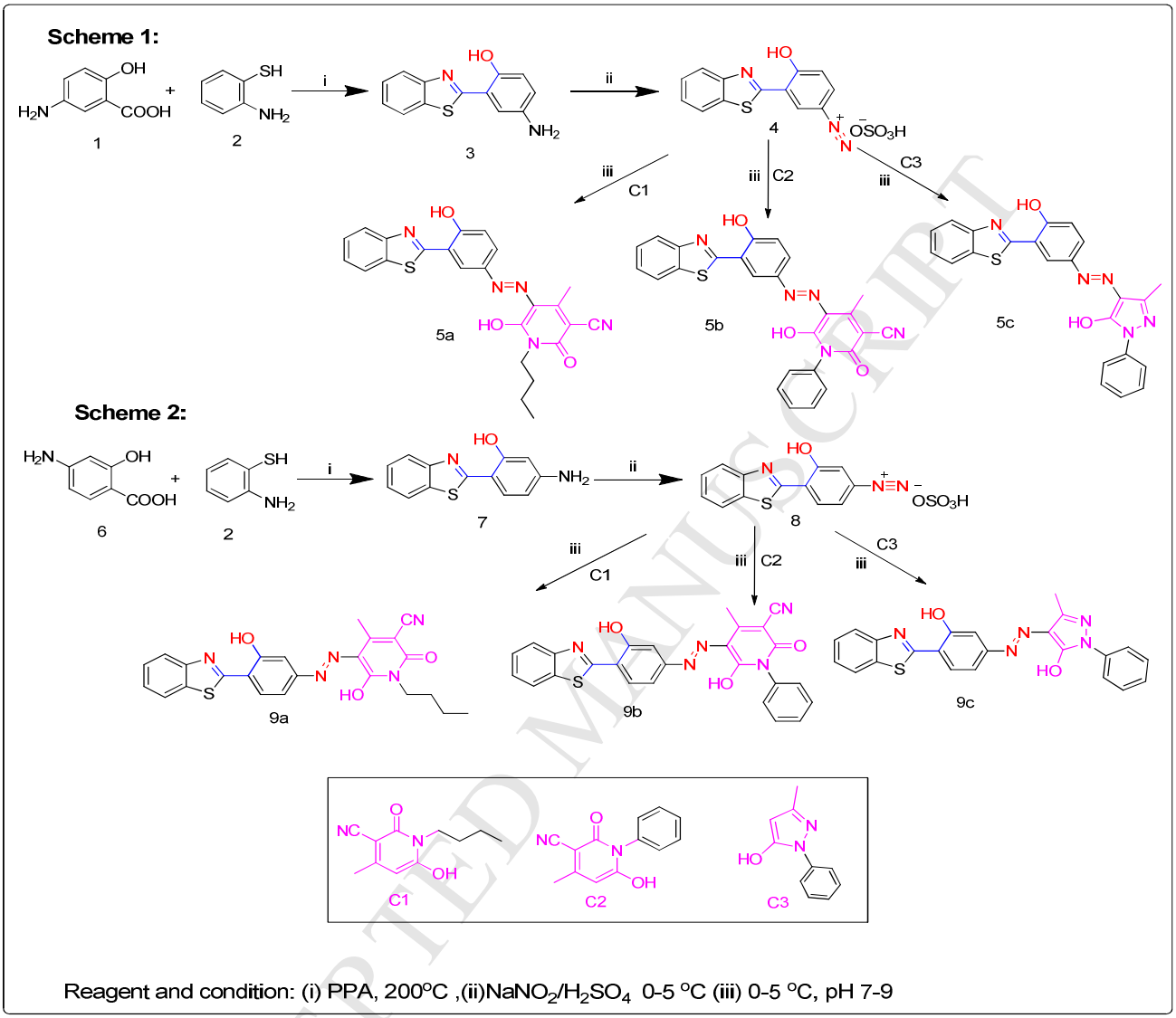

Scheme A: Synthesis scheme of new Heterocyclic Azo Dyes **5 (a-c) and 9 (a-c)**.

3. Results and discussions

Six new heterocyclic azo dyes containing benzothiazole moiety are successfully synthesized according to **scheme A**. Intermediates **3** and **7** are prepared via cyclisation, by reacting of 5-aminosalicylic acid or 4-aminosalicylic acid with 2-aminothiophenol respectively. These intermediates **3** or **7** were treated with conc. H_2SO_4 and sodium nitrite ($NaNO_2$) at 0-5 ^oC to obtain the diazonium salt solution and then coupled with compounds **C1** or **C2** or **C3** at 0-5 ^oC by maintaining pH 7-9. The desired new heterocyclic dyes **5(a-c)** and **9(a-c)** were obtained in good yield.

3.1 Characterization

3.1.1 In the "IR spectra" of **5(a-c)** and **9(a-c),** a broad peak observed around 3270 cm^{-1} to 3600 cm^{-1} and assigned for (-OH) stretching . Peaks observed between 1500-1550 cm^{-1} are due to azo group, (-N=N-) stretching vibrations. The "aromatic C–H stretching" vibrations were observed between 3060–3170 cm^{-1}.

3.1.2 ^{1}H NMR spectra, of **5(a-c)** and **9(a-c)** are analyzed in DMSO (d^6). Multiplet peaks in the range of 7.14-8.45 ppm shown the presence of aromatic ring protons. In all the dyes, **5(a-c)** and **9(a-c)**, two singlets peaks in the 11-14 ppm region, are due to presence of hydroxyl proton. For **5a** and **9a**, peaks are observed in the 0.9-2.7 ppm region, shows the presence of aliphatic protons. Singlet peak for three protons observed around 2.30 ppm to 2.50 ppm confirms presence of (Ar-CH_3)

3.1.3 UV-Visible and fluorescence study

A "UV-visible spectra" of **5(a-c)** or **9(a-c)** was measured in ethyl acetate as a solvent at a concentration of 10 µM in the wavelength range of 350-700 nm. The λ_{max} range for reported azo compounds is 414-457 nm. Emission spectra also measured in ethyl acetate solvent. All the azo compounds are emissive in the wavelength range of 495-561 nm and stoke's shift in the range of 79-105 nm. Pyrazole containing compounds (**5c** and **9c**) are less emissive than Pyridone compounds (**5a, 5b, 9a, 9b**). All the data is summarized in **Table 1.**

Table 1: Absorption and emission spectral data for **5(a-c)** and **9(a-c)**

Compound	Absorbance		Emission		Stoke's shift	
	(nm)	(cm^{-1})	(nm)	(cm^{-1})	(nm)	(cm^{-1})
5a	456	21930	559	17889	103	4041
5b	457	21881	551	18148	94	3733
5c	414	24155	495	20202	81	3953
9a	457	21882	560	17857	103	4025
9b	456	21930	561	17825	105	4105
9c	421	23753	500	20000	79	3753

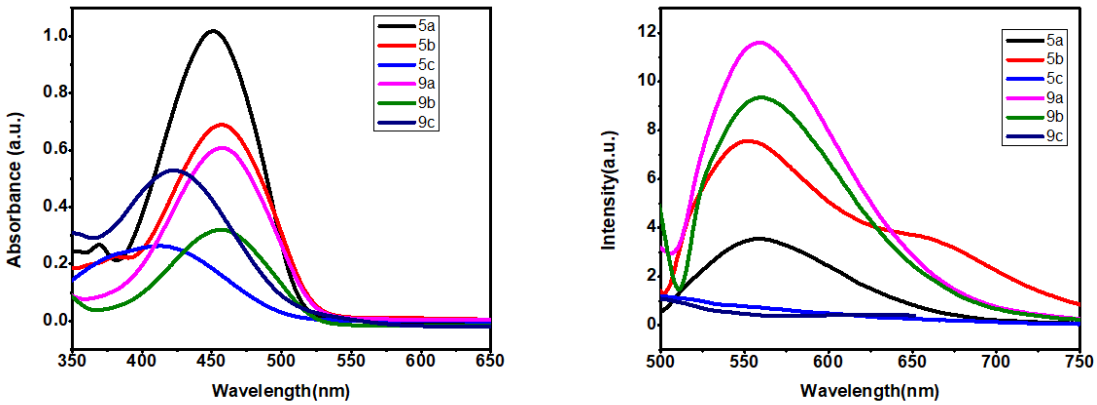

Figure.1 UV-Visible absorption and emission spectra of synthesized **5(a-c)** and **9(a-c)** in Ethyl Acetate

3.2 Biological evaluation

3.2.1 Antibacterial testing

The six newly synthesized azo compounds, **5(a-c)** and **9(a-c)** were further tested for their antimicrobial potential using the well-known "Resazurin microtiter assay method" (REMA) method. All the activities are reported in "MIC(µg/mL)" and mentioned in **Table 2**. The bacterial strains used were "gram-positive" (*S. aureus*) and "gram-negative" ("*E. coli*") bacteria. The standard "MIC values" obtained for ciprofloxacin drug were 50 µg/mL (on *S.aureus*) and 25 µg/mL (on *E.coli*) [34]. The compounds **5a** and **9c** were obtained with moderate antibacterial potential against "gram-negative" strains having "MIC values" of 312.5 µg/mL.

Table 2: The tabular representation for *in-vitro* antimicrobial activities of **5(a-c)** and **9(a-c).**

	"MIC" (µg/mL)	
Compound	**"Gram- positive" *("Staphylococcus aureus")***	**"Gram- negative" *("Escherichia coli")***
5a	1250	312.5
5b	1250	1250
5c	1250	625
9a	625	625
9b	1250	625
9c	625	312.5
Ciprofloxacin	50	25

3.2.2 Electrophoretic mobility shift assay (DNA cleavage studies)

The DNA cleavage studies carried out with the plasmid pBR 322 DNA using the Electrophoretic mobility shift assay by using the well-known protocol [35]. An increment in DNA isoforms was determined with naked eyes. When a circular plasmid DNA is run using the agarose gel electrophoresis, the fastest migration will be for supercoiled form (SC) i.e. (Form I). The slower moving open circular form (Form II) i.e. NC form will be produced, if one of the strands cleaved. A linear form (Form III) will be observed if both strands cleave and it will migrate in between SC form and NC form. Our results showed concentration-dependent formation of NC (Form II) form from SC form (Form I) (**SI, Figure S1)**. Presence of three forms of pBR322 DNA for **9b** and **9c** proved that these compounds were slightly caused double-strand DNA cleavage. There were distinguishable formations of condensed DNA forms and majority formation of Nick DNA forms (Single-stranded DNA isoform upon cleavage). The slight formation of "condensed DNA forms" may be attributed to the fact that, the compounds (with DNA complex) are enough heavy to interact and cleave both the DNA strands so that they cannot migrate across Gel- electrophoresis. Hence, observed at initial loading wells. So, we can say that compounds are inhibiting bacterial growth due to DNA cleavage i.e. interaction with their genome [36].

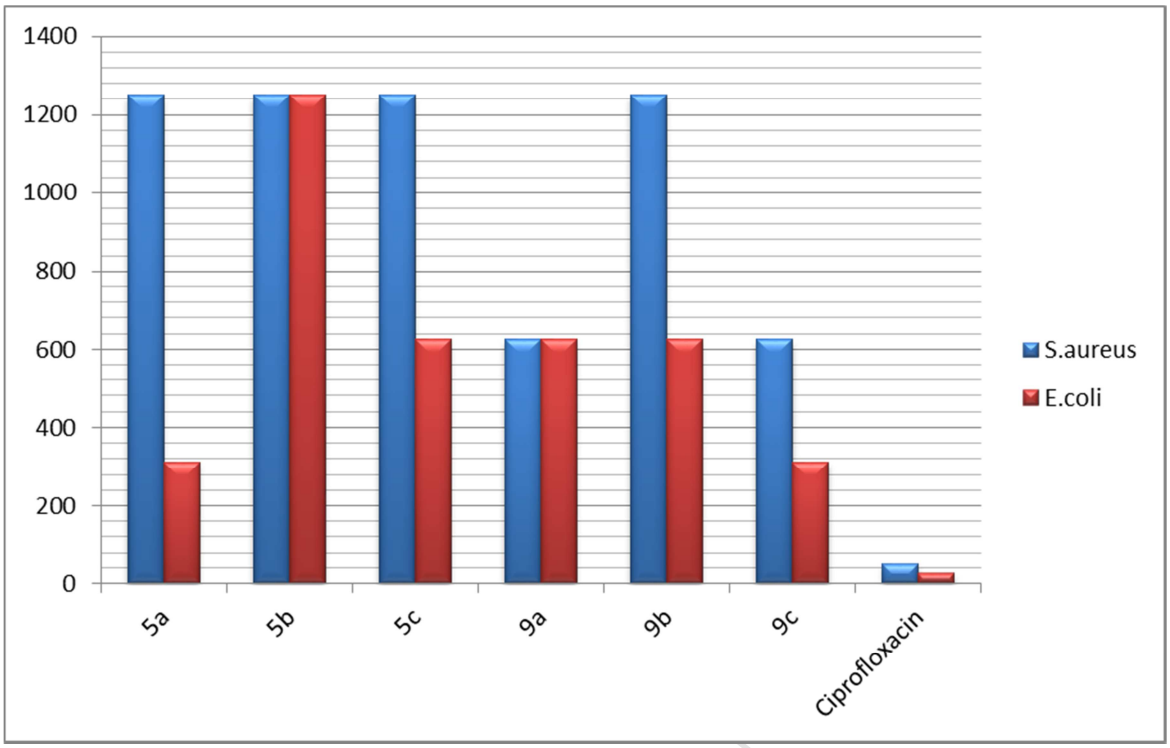

Figure 2: The plot for antibacterial activities obtained for newly synthesized azo linked compounds.

3.3 "Molecular docking" and "ADME" predictions:

The flexible ligand docking simulations were carried out using the "Glide module" [28]. The necessary 3D- crystal structure were obtained from the protein database. The crystal structures used were dialkylglycine decarboxylase (PDB id-1D7U) [37,38], "*S. aureus* Gyrase complex" with GSK299423 and DNA (PDB id:2XCS) [39] and "*S. aureus Gyrase* complex" with ciprofloxacin and DNA(PDB id:2XCT) **(Figures 3-5)**. The present six new azo compounds along with standard drug ciprofloxacin were allowed to dock into active pockets of these targets. The best dock compound, interacting residues, and their docking scores are represented in **Table 3 and 4**. The molecular mechanics generalized born surface area energy calculations were performed using the Prime module [30] **(Table 3)**. The Prime MMGBSA dG bind energy of **5c** (-60.808 kcal/mol) was better than standard ciprofloxacin (-35.625 kcal/mol). The moderate correlation between in-silico predictions and in-vitro activity data may be attributed to the number of factors like type of cell walls, pH, cell membrane permeability, environments, other metabolic reactions in bacteria, etc. which generally not considered during docking simulations. The QikProp module was incorporated for calculations of ADME parameters of these six new azo compounds **(Table 5)**. The parameters calculated from QikProp were found within acceptable ranges. The percent human oral absorption values

predicted for all these new heterocycles were more than 80%. The low-high caco-cell permeability and moderate-high logP values can be directly correlated with moderate antibacterial potential. The loose correlation between MIC may be attributed to the moderate to high caco and logP values. The changes in log P values (Lipophilicity parameter) can directly affect the passage of drug through the cell membranes. The percent human oral absorption for Standard Ciprofloxacin was found to be 48.861%; However for our compounds it is greater than standard. The in-silico predictions for ciprofloxacin showed that all the parameters for ADME are moderate and it is non-carcinogen. Accordingly, after comparing to standard ciprofloxacin, our compounds may be effectively optimized into lead compounds for potent antimicrobials agents in future. The *in-silico* carcinogenicity predictions and cytochrome profiling for compounds **5(a-c**) and **9(a-c)** (**Table 6**) were done using the admetSAR tool [39]. **Table 6** enlists the effect on various metabolic enzymes i.e. cytochromes as calculated *in-silico* using the admetSAR.

Table 3: The scores obtained after for molecular docking of compounds **5(a-c)** and **9(a-c)** on targets 2XCS, 2XCT and 1D7U.

Compound	PDB ID:2XCS		PDB ID:2XCT		PDB ID:1D7U		
	Docking score XP (Kcal/mol)	**glide energy**	**Docking score XP (Kcal/mol)**	**glide energy**	**Docking score XP (Kcal/mol)**	**glide energy**	**MMGBSA dG Bind Energy (Kcal/mol)**
5a	-2.242	-38.61	-6.277	-38.92	-2.659	-2.173	-43.162
5b	-4.048	-41.289	-5.955	-36.093	-2.711	-1.565	-40.618
5c	-4.246	-41.257	-7.353 (most dock)	-43.547	-3.745 (most dock)	-8.74	-60.808
9a	-2.593	-43.155	-4.519	-25.455	-3.008	-5.894	-40.31
9b	-4.148	-33.476	-4.355	-38.018	-	-	-
9c	-4.423 (most dock)	-43.562	-6.486	-31.834	-	-	-
Ciprofloxacin	-3.523	-41.993	-8.811	-41.855	-3.066	-12.357	-35.625

Table 4: The results for interactions obtained after molecular docking of compounds **5(a-c)** and **9(a-c)** on target proteins 2XCS, 2XCT and 1D7U.

Compound	PDB ID:2XCS	PDB ID:2XCT	PDB ID:1D7U
		INTERACTING RESIDUES	
5a	DG E:10(PI-PI STACKING)	MN G:2000(SALT BRIDGE)	ARG406(PI-CATION),LYS272(SALT BRIDGE),TRP138(H-BOND)

5b	DC F:11,DG F:10,DC E:11, DGE:10 (PI-PI STACKING),GLY D:1117(H-BOND)	MN G:2000(SALT BRIDGE)	ARG406(PI-CATION),LYS272(SALT BRIDGE,PI-CATION)
5c	DC F:11 & DG F:10(PI-PI STACKING)	MN G:2000(SALT BRIDGE), DG G:9(PI-PI STACKING), DA H:13(H-BOND)	ARG406 & LYS272(SALT BRIDGE),GLN52(H-BOND),TYR20(H-BOND),TRP123(PI-PI STACKING)
9a	LYS D:581(H-BOND)	MN G:2000(SALT BRIDGE), DG G:9,DA H:13(PI-PI STACKING)	ARG406(H-BOND),TRP138(H-BOND)
9b	DC E:11(PI-PI STACKING,H-BOND), DC F:11, DG E:10(PI-PI STACKING)	MN G:2000(SALT BRIDGE), DA H:13(PI-PI STACKING,H-BOND),DG G:9(PI-PI STACKING)	NOT DOCKED
9c	DC F:11,DG F:10, DG E:10(PI-PI STACKING)	MN G:2000(SALT BRIDGE), DA H:13,DG G:9(PI-PI STACKING)	NOT DOCKED
CIPRO-FLOXACIN	DG F:8,DG F:9(SALT BRIDGE,H-BOND)	MN G:2000(SALT BRIDGE), DA H:13,DG G:9(PI-PI STACKING)	TRP138(PI-CATION),ALA112(H-BOND)

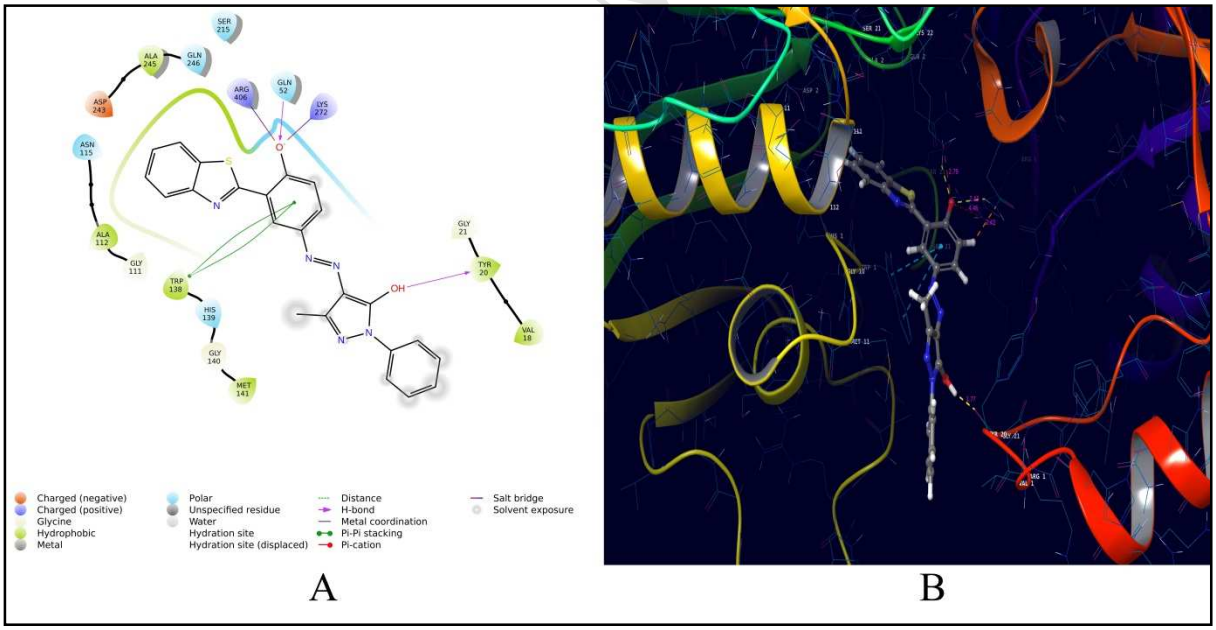

Figure 3: A] 2D and **B]** 3D interaction diagram for best dock **5c**:1D7U.

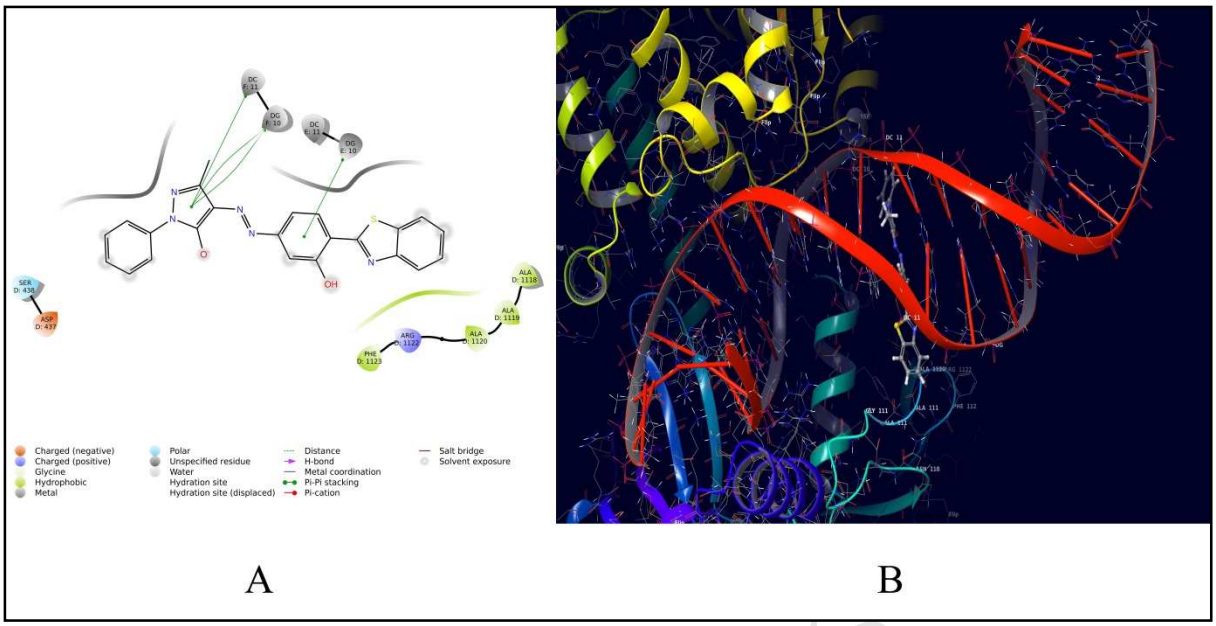

Figure 4: **A]** 2D and **B]** 3D interaction diagram for best dock **9c**:2XCS.

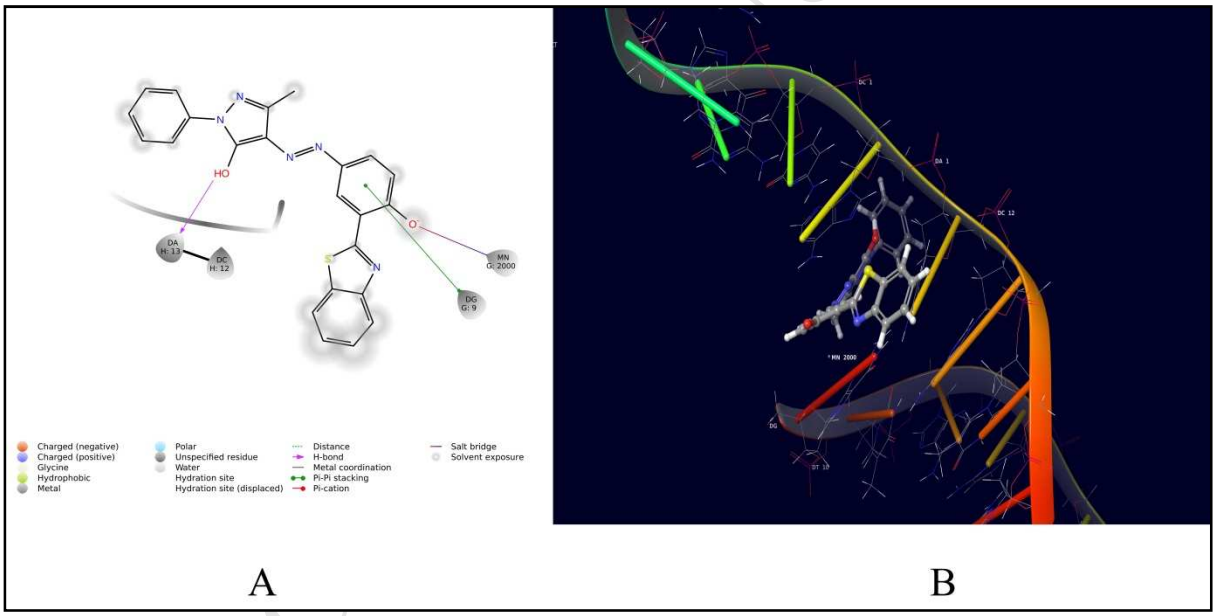

Figure 5: **A]** 2D and **B]** 3D interaction diagram for best dock **5c**:2XCT.

Table 5: ADME predictions by QikProp of **5(a-c)** and **9(a-c).**

Compound	MW	volume	QPlogPo/w	QPPCaco	#metab	%Human Oral Absorption	PSA	Rule Of Five	#stars
5a	459.52	1422.189	3.523	124.247	5	85.056	124.696	0	1
5b	479.51	1430.656	3.803	125.057	5	86.746	125.646	0	2
5c	427.48	1308.787	5.085	853.876	5	96.224	87.057	1	2
9a	459.52	1425.501	3.569	131.696	5	85.781	124.577	0	1
9b	479.51	1432.594	3.831	131.327	5	87.292	125.473	0	2
9c	427.48	1306.605	5.08	880.024	5	96.435	86.984	1	2
Ciprofloxacin	331.346	1017.742	0.28	13.583	0	48.861	98.121	0	1

#stars=Number of property or descriptor values that fall outside the 95% range of similar values for known drugs ,**QPlogPo/w** = Predicted octanol/water partition coefficient, **QPPCaco** = Predicted apparent Caco-2 cell permeability in nm/sec. , **Percent Human Oral Absorption**= Predicted human oral absorption on 0 to 100% scale., **Rule of Five**= Number of violations of Lipinski's rule of five, **volume** =Total solvent-accessible volume in cubic angstroms using a probe with a 1.4 Å radius, **PSA**= Van der Waals surface area of polar nitrogen and oxygen atoms, **#metab**=Number of likely metabolic reactions.

Table 6: *In-silico* distribution of **5(a-c)** and **9(a-c)** as obtained from the admetSAR server.

Compound	p-gp substrate/ inhibitor probability	CYP-2C9 substrate/ inhibitor	CYP-2D6 substrate/ inhibitor	CYP-3A4 substrate/ inhibitor	CYP-1A2 inhibitor	CYP-2C19 inhibitor	Rat Acute Toxicity LD50, mol/kg	Carcinogenicity
5a	Substrate /Non inhibitor	Non-substrate	Non-substrate	Substrate/inhibitor	Non-Inhibitor	Non-Inhibitor	2.4766	Non-carcinogen
5b	Non-substrate /Non inhibitor	Non-substrate	Non-substrate	Substrate/inhibitor	Non-Inhibitor	Inhibitor	2.3636	Non-carcinogen
5c	Non-substrate /Non inhibitor	Non-substrate	Non-substrate	Substrate/inhibitor	Inhibitor	Inhibitor	2.2467	Non-carcinogen
9a	Substrate /Non inhibitor	Non-substrate	Non-substrate	Substrate/inhibitor	Non-Inhibitor	Non-Inhibitor	2.4766	Non-carcinogen
9b	Non-substrate /Non inhibitor	Non-substrate	Non-substrate	Substrate/inhibitor	Non-Inhibitor	Inhibitor	2.3636	Non-carcinogen
9c	Non-substrate /Non inhibitor	Non-substrate	Non-substrate	Substrate/inhibitor	Inhibitor	Inhibitor	2.2467	Non-carcinogen
Ciprofloxacin	substrate /Non inhibitor	Non-substrate	Non-substrate	Non-substrate	Non-inhibitor	Non-inhibitor	2.1882	Non-carcinogen

3.4 Molecular Dynamics Study

The molecular dynamics simulation study was performed with OPLS-2005 force filed for 5ns (nanoseconds) simulation time with best-docked **5c**:1D7U complex using Desmond 4 module

(Schrodinger LLC, NY, release 2016). The total of 55106 atoms were present during the simulation. The trajectories were collected at every 4.8 ps and numbers of frames were kept at 250. After simulation with water as a solvent, we found that the complex was enough stable for a period of 5ns **(Figure 6-7).**

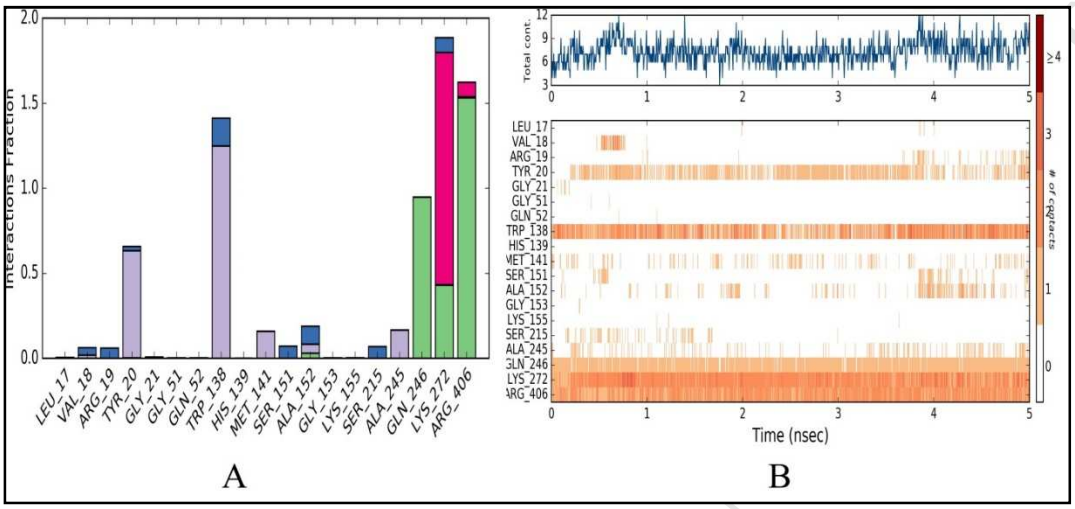

Figure- 6 A] Showing the protein-ligand interaction throughout the simulation time of 5ns (green-H-bond, purple-hydrophobic contacts, Pink-ionic contacts, and Blue-Water bridges).Values more than 1 suggesting more contacts and corresponding to 100%. **B]** Timeline representation plot after MD simulation time of 5ns.

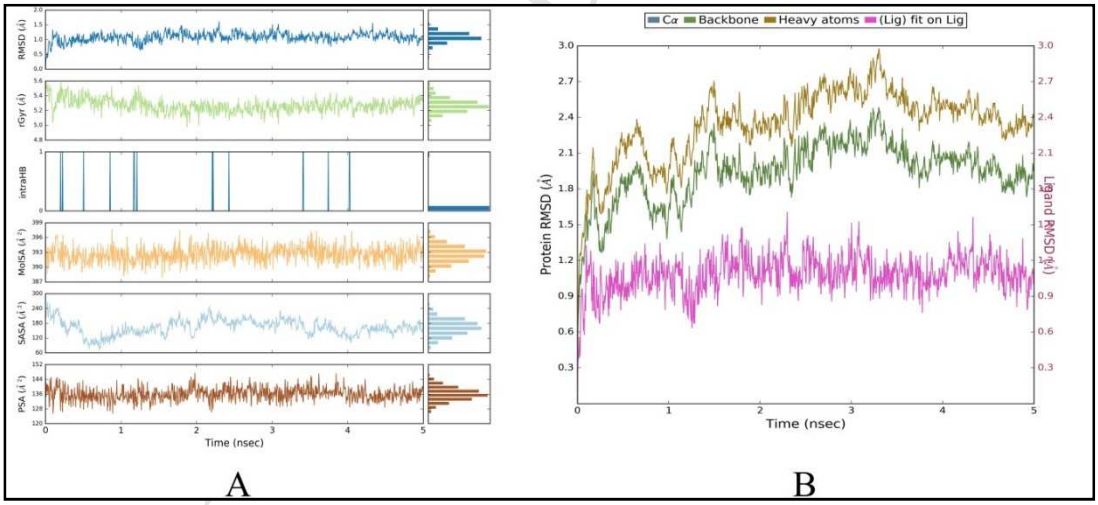

Figure-7: A] A plot showing the properties corresponding with ligands after MD simulation and **B]** RMSD plot for **5c:1D7U** complex.

3.5 "HOMO–LUMO theory" and ("FMO" approach)

All the compounds **5(a-c)** and **9(a-c)** are optimized with "B3LYP/6-31g (d)" method in the gas phase. "Highest Occupied Molecular Orbital"- i.e. "HOMO" and "Lowest Unoccupied Molecular Orbital"- i.e. "LUMO" are the most important orbitals in a molecule. Analyzing the Energy gap ($E_{LUMO} - E_{HOMO}$) is important, as these values are related to the reactivity of molecules [34]. A molecule with a high chemical reactivity and low kinetic stability is generally accomplice with a small energy gap between frontier orbitals. A molecule when energized, it easily loses an electron, as "HOMO energy" is directly related to "ionization potential". On the other hand "LUMO energy" directly related with "electron affinity", as it accepts an electron. "HOMO – LUMO" theory is used to compare with biological activities of newly synthesized dyes **5(a-c)** and **9(a-c).** The ($E_{LUMO} - E_{HOMO}$) values are gathered in **Table 7** and also presented in **Figure 8.** It is observed that **9(a-c)** has less "HOMO-LUMO" gap compared to **5(a-c).** So, **9(a-c)** should exhibit better biological activity compared to **5(a-c).** This correlation confirmed by "REMA assay method". Dyes **9(a-c)** shown comparatively better activities than dyes **5(a-c)** for "*S.aureus"* bacteria.

Table 7: The tabular representation for calculation of "HOMO-LUMO energy gap" for synthesized compounds **5(a-c)** and **9(a-c).**

	HOMO Energy		LUMO Energy		E_{LUMO}-E_{HOMO}
Compound	**Hartree**	**eV**	**Hartree**	**eV**	**eV**
5a	-0.2064	-5.61	-0.0784	-2.13	3.48
5b	-0.2050	-5.58	-0.0768	-2.09	3.49
5c	-0.1964	-5.34	-0.0634	-1.73	3.62
9a	-0.2113	-5.75	-0.0940	-2.56	3.19
9b	-0.2102	-5.72	-0.0924	-2.56	3.20
9c	-0.2029	-5.52	-0.0793	-2.16	3.36

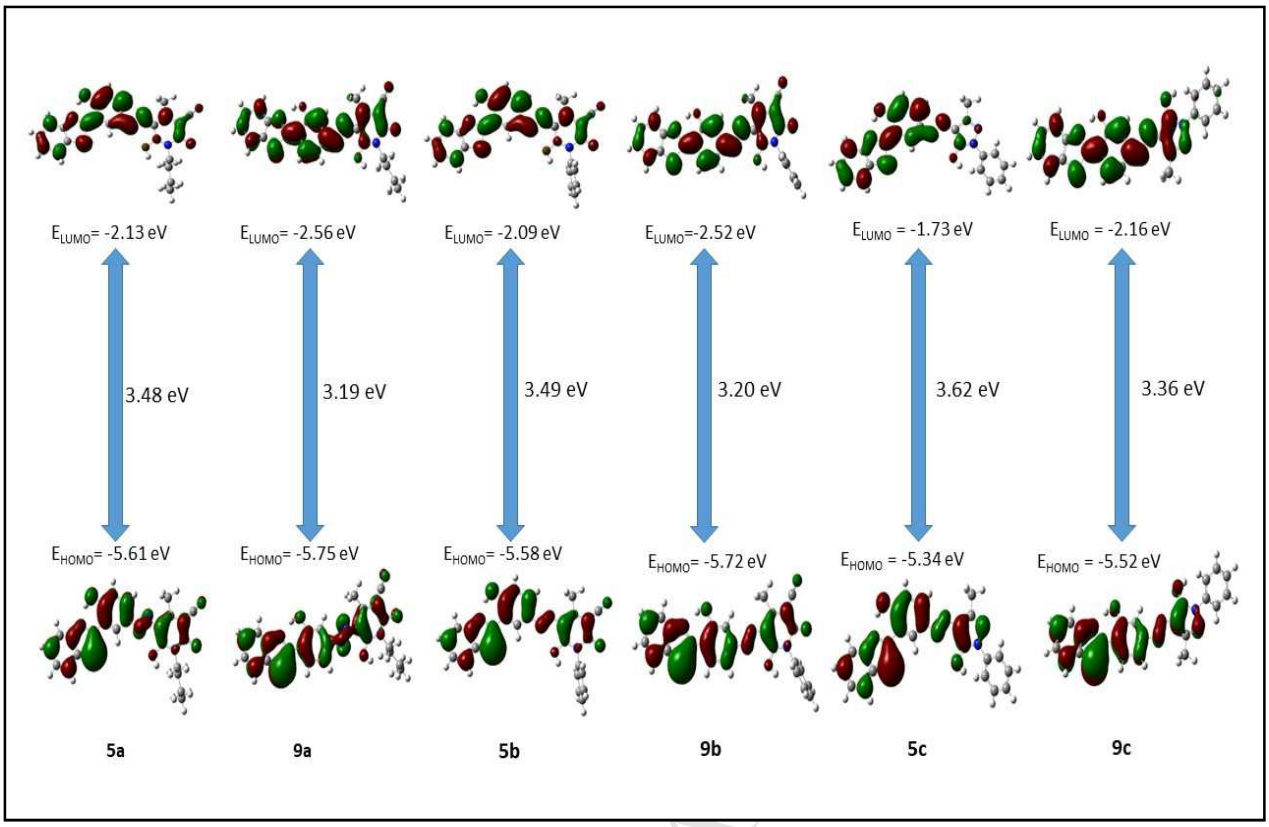

Figure 8: The graphical representation for the calculation of "HOMO-LUMO energy gap" for **5(a-c)** and **9(a-c).**

4. Conclusion

In the present work, six new **5(a-c)** and **9(a-c)** heterocyclic azo compounds are synthesized. These azo clubbed derivatives were characterized using various spectroscopic techniques such as ^{1}H NMR, FTIR, UV–Visible, fluorescence spectroscopy, LC-MS, and elemental analysis. All compounds are emissive and shown Stoke's shifts of around 81-105nm. All compounds are screened against antibacterial activity by using REMA method. **5a** and **9a** showed moderate activity against Gram-negative *(Escherichia coli)* strain. Comparative HOMO-LUMO studies also performed and it observed that **9(a-c)** molecules have less HOMO-LUMO gap compared to **5(a-c).** Compounds which have comparative less HUMO-LUMO gap shown good activity. Molecular docking protocols were performed for different target proteins (PDB ids-2XCS, 2XCT, and 1D7U).The results after docking studies were correlated with the actual *in-vitro* data. Molecular Dynamics Study showed that the complex was stable for common bacterial target protein 1D7U complex with most docked molecule **5c** during 5 ns simulation time. In summary, our studies indicated that these complexes have an affinity for DNA. Furthermore, the docking simulation results obtained in present work suggests the future applications of these azo clubbed compounds as antibacterial agents.

Accordingly, after comparing ADME and molecular properties of our compounds to standard ciprofloxacin, our compounds may be effectively optimized into lead compounds for potent antimicrobial agents in future.

Acknowledgment

Authors (CWG and VRM) are thankful to Principal Scientific Adviser to Government of India (PSA to GOI) for JRF (Junior Research Fellowship) and financial support.

5. References:

[1] J.J.S.-G. Krasaka, Synthesis and Properties of Monoazo Disperse Dyes Derived from 3-Amino-5-nitro [2,1] benzisothiazole, Dye. Pigment. 8 (1987) 345–352. doi:10.1016/0143-7208(87)85024-6.

[2] M.A. Satam, R.K. Raut, N. Sekar, Dyes and Pigments and comparison with 2-naphthol analogs, Dye. Pigment. 96 (2013) 92–103. doi:10.1016/j.dyepig.2012.07.019.

[3] S.K. Lanke, N. Sekar, Coumarin Push-Pull NLOphores with Red Emission: Solvatochromic and Theoretical Approach, J. Fluoresc. 26 (2016) 949–962. doi:10.1007/s10895-016-1783-6.

[4] M.M. Jadhav, I.A. Alswaidan, L. Rhyman, P. Ramasami, N. Sekar, TD-DFT Investigation of 2,5-Bis(2-benzothiazolyl)hydroquinone and 2,5-Bis(benzo[d]thiazol-2-yl)-4-methoxyphenol, J. Solution Chem. 46 (2017) 1005–1023. doi:10.1007/s10953-017-0628-5.

[5] T. Tao, F. Xu, X.C. Chen, Q.Q. Liu, W. Huang, X.Z. You, Comparisons between azo dyes and Schiff bases having the same benzothiazole/phenol skeleton: Syntheses, crystal structures and spectroscopic properties, Dye. Pigment. 92 (2012) 916–922. doi:10.1016/j.dyepig.2011.09.008.

[6] J. Graham, C.E. Wong, J. Day, E. McFaddin, U. Ochsner, T. Hoang, C.L. Young, W. Ribble, M.A. DeGroote, T. Jarvis, X. Sun, Discovery of Benzothiazole Amides as Potent Antimycobacterial Agents, Bioorg. Med. Chem. Lett. (2018) 1–5. doi:10.1016/j.bmcl.2018.08.026.

[7] S.K. Maddili, Z.Z. Li, V.K. Kannekanti, R.R.Y. Bheemanaboina, B. Tuniki, V.K.R. Tangadanchu, C.H. Zhou, Azoalkyl ether imidazo[2,1-b]benzothiazoles as potentially antimicrobial agents with novel structural skeleton, Bioorganic Med. Chem. Lett. 28 (2018) 2426–2431. doi:10.1016/j.bmcl.2018.06.016.

[8] A. Rouf, C. Tanyeli, Bioactive thiazole and benzothiazole derivatives, Eur. J. Med. Chem. 97 (2015) 911–927. doi:10.1016/j.ejmech.2014.10.058.

[9] P.C. Sharma, A. Sinhmar, A. Sharma, H. Rajak, D.P. Pathak, Medicinal significance of benzothiazole scaffold: An insight view, J. Enzyme Inhib. Med. Chem. 28 (2012) 240–266. doi:10.3109/14756366.2012.720572.

[10] M.T. El Sayed, M.A.M.S. El-Sharief, E.S. Zarie, N.M. Morsy, A.R. Elsheakh, A. Voronkov, V. Berishvili, G.S. Hassan, Design, synthesis, anti-inflammatory activity and molecular docking of potential novel antipyrine and pyrazolone analogs as cyclooxygenase enzyme (COX) inhibitors, Bioorganic Med. Chem. Lett. 28 (2018) 952–957. doi:10.1016/j.bmcl.2018.01.043.

[11] S. Rasapalli, Y. Fan, M. Yu, C. Rees, J.T. Harris, J.A. Golen, J.P. Jasinski, A.L. Rheingold, S.M. Kwasny, T.J. Opperman, Detour of prenostodione synthesis towards pyrazolones for antibacterial activity, Bioorganic Med. Chem. Lett. 23 (2013) 3235–

3238. doi:10.1016/j.bmcl.2013.03.123.
[12] D. Renck, P. Machado, A.A. Souto, L.A. Rosado, T. Erig, M.M. Campos, C.B. Farias, R. Roesler, L.F.S.M. Timmers, O.N. De Souza, D.S. Santos, L.A. Basso, Design of Novel Potent Inhibitors of Human Uridine Phosphorylase- 1: Synthesis, Inhibition Studies, Thermodynamics, and in Vitro In fl uence on 5 □ Fluorouracil Cytotoxicity, 56 (2013) 8892–8902. doi:10.1021/jm401389u.
[13] V.A. Joseph, J.H. Pandya, R.N. Jadeja, Syntheses , crystal structure and biological evaluation of Schiff bases and copper complexes derived from 4-formylpyrazolone, J. Mol. Struct. 1081 (2015) 443–448. doi:10.1016/j.molstruc.2014.10.056.
[14] V. Kumar, K. Kaur, G. Kumar, A. Kumar, European Journal of Medicinal Chemistry Pyrazole containing natural products : Synthetic preview and biological signifi cance, Eur. J. Med. Chem. 69 (2013) 735–753. doi:10.1016/j.ejmech.2013.08.053.
[15] F. Karc, F. Karc, A. Demirçal, M. Yamaç, Synthesis , solvatochromic properties and antimicrobial activities of some novel pyridone-based disperse disazo dyes, J. Mol. Liq. 187 (2013) 302–308. doi:10.1016/j.molliq.2013.08.005.
[16] Y. Cui, G. Qian, L. Chen, Z. Wang, M. Wang, Synthesis and nonlinear optical properties of a series of azo chromophore functionalized alkoxysilanes, Dye. Pigment. 77 (2008) 217–222. doi:10.1016/j.dyepig.2007.05.005.
[17] M.S. Refat, M.Y. El-sayed, A. Majid, A. Adam, Cu (II), Co (II) and Ni (II) complexes of new Schiff base ligand : Synthesis , thermal and spectroscopic characterizations, J. Mol. Struct. 1038 (2013) 62–72. doi:10.1016/j.molstruc.2013.01.059.
[18] F. Qiu, Y. Cao, H. Xu, Y. Jiang, Synthesis and properties of polymer containing azo-dye chromophores for nonlinear optical applications, Dye. Pigment. 75 (2007) 454–459. doi:10.1016/j.dyepig.2006.06.037.
[19] B. Çatikkaş, E. Aktan, E. Yalçin, Vibrational and electronic investigations, NLO, FMO analysis on a hetarylazoindole disperse dye by density functional theory, J. Mol. Struct. 1117 (2016) 218–226. doi:10.1016/j.molstruc.2016.03.074.
[20] V.R. Mishra, C.W. Ghanavatkar, S.I. Qureshi, H.K. Chaudhari, N. Sekar, Design, Synthesis, antimicrobial activity and computational studies of novel azo linked substituted benzimidazole, benzoxazole and benzothiazole derivatives, Comput. Biol. Chem. 78 (2019) 330–337. doi:10.1016/j.compbiolchem.2019.01.003.
[21] N. Hassan, A.Z. El-sonbati, M.G. El-desouky, Synthesis , characterization , molecular docking and DNA binding studies of Cu (II), Ni (II), Zn (II) and Mn (II) complexes, J. Mol. Liq. 242 (2017) 293–307. doi:10.1016/j.molliq.2017.07.019.
[22] W.H. Mahmoud, G.G. Mohamed, S.Y.A. Mohamedin, Spectroscopic characterization, thermal, antimicrobial and molecular docking studies on nano-size mixed ligand complexes based on sudan III azodye and 1,10-phenanthroline, J. Therm. Anal. Calorim. 130 (2017) 2167–2184. doi:10.1007/s10973-017-6482-2.
[23] W.H. Mahmoud, F.N. Sayed, G.G. Mohamed, Synthesis, characterization and *in vitro* antimicrobial and anti-breast cancer activity studies of metal complexes of novel pentadentate azo dye ligand, Appl. Organomet. Chem. 30 (2016) 959–973. doi:10.1002/aoc.3529.
[24] A. Mohammadi, B. Khalili, M. Tahavor, Novel push-pull heterocyclic azo disperse dyes containing piperazine moiety: Synthesis, spectral properties, antioxidant activity and dyeing performance on polyester fibers, Spectrochim. Acta - Part A Mol. Biomol. Spectrosc. 150 (2015) 799–805. doi:10.1016/j.saa.2015.06.024.
[25] S.N. Mali, H.K. Chaudhari, Computational Studies on Imidazo[1,2-a] Pyridine-3-Carboxamide Analogues as Antimycobacterial Agents: Common Pharmacophore Generation, Atom-based 3D-QSAR, Molecular dynamics Simulation, QikProp,

Molecular Docking and Prime MMGBSA Approaches, Open Pharm. Sci. J. 5 (2018) 12–23. doi:10.2174/1874844901805010012.

[26] G. M. J. Frisch, W. Trucks, H.B. Schlegel, G.E. Scuseria, M.A. Robb, J.R. Cheeseman, G. Scalmani, V. Barone, B. Mennucci, G.A. Petersson, H. Nakatsuji, M. Caricato, X. Li, H.P. Hratchian, A.F. Izmaylov, J. Bloino, G. Zheng, J.L. Sonnenberg, Gaussian 09, Revision C.01, Inc. Wallingford, CT. (2009) 2009–2009. doi:111.

[27] A.D. Becke, A new mixing of Hartree–Fock and local density-functional theories, J. Chem. Phys. 98 (1993) 1372. doi:10.1063/1.464304.

[28] C. Lee, W. Yang, R.G. Parr, Development of the Colic-Salvetti correlation-energy into a functional of the electron density formula Chengteh, Phys. Rev. B. 37 (1988) 785–789. doi:10.1103/PhysRevB.37.785.

[29] Glide., New York, NY:Schrodinger, LLC, (2017).

[30] Qikprop, New York, NY: Schrodinger, LLC, (2017).

[31] Prime., New York, NY: Schrodinger, LLC, (2017).

[32] M.G. Holler, L.F. Campo, A. Brandelli, V. Stefani, Synthesis and spectroscopic characterisation of 2-(2′-hydroxyphenyl)benzazole isothiocyanates as new fluorescent probes for proteins, J. Photochem. Photobiol. A Chem. 149 (2002) 217–225. doi:10.1016/S1010-6030(02)00008-4.

[33] C.C. Chen, I.J. Wang, Synthesis of some pyridone azo dyes from 1-substituted 2-hydroxy-6-pyridone derivatives and their colour assessment, Dye. Pigment. 15 (1991) 69–82. doi:10.1016/0143-7208(91)87008-B.

[34] P.M. Chauhan, S.N. Thummar, K.H. Chikhalia, Design, synthesis, bioactivity, and computational studies of some morpholine-clubbed coumarinyl acetamide and cinnamide derivatives, J. Iran. Chem. Soc. 15 (2018) 1261–1277. doi:10.1007/s13738-018-1324-0.

[35] S.S. Bhat, N. Shivalingegowda, V.K. Revankar, N.K. Lokanath, M.S. Kugaji, V. Kumbar, K. Bhat, Synthesis, structural characterization and biological properties of phosphorescent iridium(III) complexes, J. Inorg. Biochem. 177 (2017) 127–137. doi:10.1016/j.jinorgbio.2017.09.020.

[36] N.M. Mallikarjuna, J. Keshavayya, Synthesis, spectroscopic characterization and pharmacological studies on novel sulfamethaxazole based azo dyes, J. King Saud Univ. - Sci. (2018). doi:10.1016/j.jksus.2018.04.033.

[37] V.N. Malashkevich, P. Strop, J.W. Keller, J.N. Jansonius, M.D. Toney, Crystal structures of dialkylglycine decarboxylase inhibitor complexes, J. Mol. Biol. 294 (1999) 193–200. doi:10.1006/jmbi.1999.3254.

[38] F.A. Bassyouni, T.S. Saleh, M.M. Elhefnawi, S.I.A. El-Moez, W.M. El-Senousy, M.E. Abdel-Rehim, Synthesis, pharmacological activity evaluation and molecular modeling of new polynuclear heterocyclic compounds containing benzimidazole derivatives, Arch. Pharm. Res. 35 (2012) 2063–2075. doi:10.1007/s12272-012-1204-6.

[39] B.D. Bax, P.F. Chan, D.S. Eggleston, A. Fosberry, D.R. Gentry, F. Gorrec, I. Giordano, M.M. Hann, A. Hennessy, M. Hibbs, J. Huang, E. Jones, J. Jones, K.K. Brown, C.J. Lewis, E.W. May, M.R. Saunders, O. Singh, C.E. Spitzfaden, C. Shen, A. Shillings, A.J. Theobald, A. Wohlkonig, N.D. Pearson, M.N. Gwynn, Type IIA topoisomerase inhibition by a new class of antibacterial agents, Nature. 466 (2010) 935–940. doi:10.1038/nature09197.

Synthesis, Bioactivities, DFT and *in-silico* appraisal of azo clubbed Benzothiazole derivatives.

.

Chaitannya W. Ghanavatkar[a], Virendra R. Mishra[a], Suraj N. Mali[b]. Dr. Hemchandra K. Chaudhari[b], Nagaiyan Sekar[a, *]

Highlights

- Six new heterocyclic azo dyes are synthesised
- They are emissive, showed Stoke's shifts of around 81-105nm
- They have moderate activity against Gram-negative *(Escherichia coli)* strain. DFT-computed HOMO-LUMO studies also performed.
- Docking studies on common bacterial targets (PDB ids-2XCS, 2XCT and 1D7U) showed good results
- Molecular Dynamics studies showed that the complex was stable for common bacterial target protein 1D7U complex with most docked molecule **5c** during 5ns simulation time.
- These complexes have moderate affinity for DNA.